ANNALES
UNIVERSITATIS MARIAE CURIE-SKŁODOWSKA
LUBLIN — POLONIA
VOL. XLV, 10 SECTIO AAA 1990

Instytut Fizyki UMCS

Bożena NERLO-POMORSKA, Beata SKORUPSKA

Shapes and Sizes of Nuclei with $50 < Z, N < 80$[1]

Kształt i rozmiary jąder o $50 < Z, N < 80$

INTRODUCTION

The neutron deficient nuclei with $50 < Z, N < 80$ nucleon numbers have been already investigated theoretically [1,2] but the last development of the laser measurement techniques [3,4] as well as the new possibilities of the microscopic analysis enable now the better explanation of the diversing sizes and shapes mechanisms in this region. The Te-Gd isotopes far from the β stability line show some interesting features. They are well deformed, with the deformation energy up to ~ 10 MeV. Their potential energy reaches minimal values not only for the prolate shapes but also for the oblate ones, especially for isotopes with $N > 74$. They have also some hexadecapole deformation at the equilibrium point [5].

For a long time there was a shortage of the single-particle levels scheme parameters here. The extrapolated from the rare earth and actinide regions, Nilsson potential parameters, were not sufficient to describe the subtle effects in the neutron deficient nuclei. Now we have used the universal set of parameters [6] depending only on the average mass number of the whole region: A $\sim$ 126 in our case.

We have performed the dynamical calculation on the basis of the collective hamiltonian, obtained in the generator coordinate method (GCM). This hamiltonian consists of the GCM mass parameters and the potential

[1] Paper supported by the Polish Ministry of Education, project CPBP 01.09.

energy improved by the zero point correction term. The many-body hamiltonian used here contains in spite of the Nilsson type single particle hamiltonian the pairing interaction and the long range two-body forces in the local approximation [7]. The quadrupole (ϵ) and hexadecapole (ϵ_4) deformation parameters are taken as generator coordinates, and BCS ground state as the generator function. The BCS wave function was approximately projected on a good particle number [8] and the average strength of pairing forces was taken from ref. [9].

We have calculated the potential energy surfaces, equilibrium deformations, mass parameters and dynamical multipole moments $Q_\lambda(\lambda = 0,2,4)$ for all the even-even nuclei with nucleon numbers $50 < Z < 80$, $Z \leq N < 80$. The chief points of the theory are presented in chapter 1. The numerical results of the calculation are illustrated in section 2. As the isotopic shifts of the mean square radius do not agree with the experimental data the more accurate investigation of their pairing and deformation parameters dependence is presented in chapter 3. The conclusions and proposals of further investigations are drawn in the last part of the paper.

THEORETICAL MODEL

The calculation was done on the two dimensional grid of deformation parameters $-0.4 \leq \epsilon_2 = \epsilon \leq 0.5, -0.12 \leq \epsilon_4 \leq 0.12$.

The single particle (hamiltonian $\hat{H}_{\rm sp}$) eigen problem was solved with the Nilsson potential with the new correction term parameters proposed by Seo in [6] $\kappa_0 = 0.021, \kappa_1 = 0.90, \gamma_0 = 0.062$

$$\hat{H}_{\rm sp}|\eta\rangle = e_\eta|\eta\rangle. \tag{1}$$

The many body hamiltonian $\hat{H}$ consists of the mean field hamiltonian $\hat{H}_0$ of Nilsson type taken in the given grid points $\{\epsilon_\gamma\} = \{\epsilon, \epsilon_4\}$, the pairing forces and the long range two body correlations in local approximation [10]

$$\hat{H} + \hat{H}_0(\{\epsilon_\lambda\}) - \frac{1}{2}\sum_{\mu,\nu=2,4} \chi_{\mu\nu}\langle\hat{F}_\mu\rangle\hat{F}_\nu - G(\langle\hat{S}^+\rangle\hat{S} + \langle\hat{S}\rangle\hat{S}^+), \tag{2}$$

where

$$\hat{H}_0 = \sum_\eta e_\eta C_\eta^+ C_\eta \tag{3}$$

with the C_η, C_η^+ fermion annihilation and creation operators.

The strength of the long range forces $\chi_{\mu\nu}$ is obtained from the selfconsistency condition

$$\chi_{\mu\nu}^{-1} = -\frac{\partial\langle a \mid \widehat{F}_{\mu} \mid a\rangle}{\partial\epsilon_{\nu}} \mid_{\{\epsilon_{\lambda}\}} . \tag{4}$$

The $\widehat{F}_{\nu}$ operators are taken in the form

$$\widehat{F}_{\nu}(\{\epsilon_{\lambda}\}) = \frac{\partial\widehat{H}_0}{\partial\epsilon_{\nu}} \mid_{\epsilon_{\lambda}} - \langle a \mid \frac{\partial\widehat{H}_0}{\partial\epsilon_{\nu}} \mid a\rangle \mid_{\epsilon_{\lambda}} . \tag{5}$$

The operator $\widehat{S}$ is

$$\widehat{S} = \sum_{\eta} C_{\eta}^{+} C_{-\eta}^{+}$$

The pairing strengths for protons (G_p) and neutrons (G_n) are equal

$$G_p Z^{2/3} = G_n N^{2/3} = 0.29\,\hbar\,\mathring{\omega}_0 . \tag{6}$$

The eigen-function of the hamiltonian (2) is approximated by the BCS wave function depending on the single particle coordinates $\{x\}$ and parametrically on the collective ones a:

$$|a\rangle = |a, \{x\}\rangle = \prod_{\eta}(U_{\eta} + V_{\eta} C_{\eta}^{+} C_{-\eta}^{+}|0\rangle, \tag{7}$$

where V_{η}^2 is the pair occupation probability, $U_{\eta}^2 = 1 - V_{\eta}$, $|0\rangle$ is the particle vacuum state. The function $|a\rangle$ will be used as a generator function and the deformation parameters are taken as the collective generator coordinates $a_1 = \epsilon, a_2 = \epsilon_4$.

The collective hamiltonian $\widehat{\mathcal{H}}_{\text{coll}}$ is given in the generator coordinate method as

$$\widehat{\mathcal{H}}_{\text{coll}} = \widehat{\mathcal{T}} + \widehat{\mathcal{V}}. \tag{8}$$

The kinetic term $\widehat{\mathcal{T}}$ is

$$\widehat{\mathcal{T}} = -\frac{1}{2\sqrt{\det\gamma}}\frac{\partial}{\partial a_i} 2\sqrt{\det\gamma}(B^{-1})^{il}\frac{\partial}{\partial a_l}, \tag{9}$$

where the mass parameters are

$$(B^{-1})^{il} = \frac{1}{2}\sum_{jk}(\gamma^{ij})_j^{-1} h_k (\gamma^{kl})^{-1} \tag{10}$$

The tensor overlap width is

$$\gamma_{ij} = \langle a| \frac{\overleftarrow{\partial}}{\partial a_i}\frac{\overrightarrow{\partial}}{\partial a_j} |a\rangle \tag{11}$$

Tab. 1. The equilibrium features of the even-even nuclei with $50 < Z < 80$, $Z \leq N < 80$

Z	N	A	ϵ^0	ϵ_4^0	V MeV	E_{def} MeV	Q_0 b	$\partial\langle r^2\rangle$ fm^2	$\partial\langle r^2\rangle^{exp}$ fm^2	$\langle Q_2^2\rangle$ b	$\sqrt{\langle Q_2^2\rangle}$ b	Q_2^{exp} b	$B2$ e^{2}b^2	$\overline{B2}$ e^{2}b^2	$B2^{exp}$ e^{2}b^2	$\langle Q_4\rangle$ b^2
52	52	104	-0.002	0.011	-11.739	-0.039	10.30	0.00		0.11	1.01		0.0012	0.1015		0.01
52	54	106	-0.026	0.003	-8.445	-0.045	10.47	0.33		0.19	1.12		0.0036	0.1248		0.05
52	56	108	-0.047	0.001	-5.901	-0.101	10.60	0.25		0.37	1.25		0.0136	0.1554		0.06
52	58	110	-0.061	0.003	-3.915	-0.215	10.72	0.23		0.55	1.44		0.0301	0.2063		0.08
52	60	112	-0.097	-0.001	-2.602	-0.201	10.86	0.27		0.70	1.66		0.0487	0.2741		0.11
52	62	114	0.194	-0.028	-1.990	-0.590	11.02	0.31		1.11	2.05		0.1226	0.4180		0.15
52	64	116	0.196	-0.015	-1.576	-0.676	11.13	0.21		1.24	2.16		0.1529	0.4641		0.14
52	66	118	-0.173	0.002	-1.768	-1.068	11.28	0.29		1.23	2.20		0.1505	0.4814		0.12
52	68	120	-0.178	0.011	-2.175	-1.275	11.39	0.21		1.06	2.05	2.78	0.1118	0.4180	0.770	0.10
52	70	122	-0.168	0.011	-2.767	-1.367	11.50	0.21	[3]	0.65	1.84	2.576	0.0420	0.3368	0.660	0.07
52	72	124	-0.130	0.014	-3.546	-0.946	11.61	0.21		0.50	1.52	2.39	0.0249	0.2298	0.568	0.04
52	74	126	-0.107	0.018	-4.790	-0.490	11.70	0.17	0.081	0.31	1.30	2.185	0.0096	0.1681	0.475	0.02
52	76	128	-0.012	-0.007	-6.622	-0.022	11.80	0.19	0.055	0.09	1.12	1.962	0.0008	0.1248	0.383	0.02
52	78	130	0.003	-0.005	-9.413	-0.013	11.90	0.19	0.047	0.01	0.97	1.722	0.0000	0.0936	0.295	0.03
54	54	108	0.138	-0.039	-5.338	-0.138	11.03	0.00		0.75	1.58		0.0560	0.2483		0.13
54	56	110	0.155	-0.030	-3.742	-0.942	11.21	0.33		1.53	2.09		0.2329	0.4345		0.20
54	58	112	0.176	-0.026	-2.497	-1.697	11.39	0.33		2.45	2.82		0.5971	0.7910		0.31
54	60	114	0.206	-0.023	-1.810	-2.310	11.59	0.37	[4]	3.16	3.45		0.9933	1.1840		0.41
54	62	116	0.217	-0.020	-1.339	-2.839	11.77	0.33		3.52	3.76		1.2325	1.4063		0.43
54	64	118	0.227	-0.003	-1.218	-3.118	11.90	0.24	0.199	3.60	3.84	3.76	1.2892	1.4668	1.40	0.39
54	66	120	0.236	0.012	-1.181	-3.281	12.02	0.22	0.097	3.71	3.94	3.07	1.3691	1.5442	0.94	0.35
54	68	122	0.229	0.017	-1.198	-2.998	12.13	0.20	0.064	3.54	3.77	3.35	1.2465	1.4138	1.12	0.27
54	70	124	0.208	0.018	-1.403	-2.602	12.22	0.17	0.057	3.20	3.45	3.87	1.0186	1.1840	1.49	0.22
54	72	126	0.178	0.009	-2.069	-2.069	12.27	0.09	0.049	2.46	2.76	2.782	0.6020	0.7577	0.77	0.15
54	74	128	0.153	0.014	-3.079	-1.479	12.34	0.13	0.041	1.70	2.18	2.74	0.2875	0.4727	0.75	0.07
54	76	130	-0.113	0.020	-4.474	-0.474	12.42	0.15	0.035	0.31	1.48	2.56	0.0096	0.2179	0.65	0.04
54	78	132	-0.009	-0.004	-6.713	-0.013	12.51	0.17	0.032	-0.04	1.20	2.15	0.0002	0.1432	0.46	0.02

Z	N	A	ϵ^0	ϵ_4^0	V MeV	E_{def} MeV	Q_0 b	$\partial\langle r^2\rangle$ fm^2	$\partial\langle r^2\rangle^{exp}$ fm^2	$\langle Q_2^2\rangle$ b	$\sqrt{\langle Q_2^2\rangle}$ b	Q_2^{exp} b	$B2$ e^{2}b^2	$\overline{B2}$ e^{2}b^2	$B2^{exp}$ e^{2}b^2	$\langle Q_4\rangle$ b^2
56	56	112	0.182	−0.014	−2.421	−2.121	11.85	0.00		2.92	3.24		0.8481	1.0442		0.34
56	58	114	0.233	−0.040	−1.543	−3.043	12.12	0.48		3.99	4.23		1.5836	1.7798		0.61
56	60	116	0.261	−0.040	−1.628	−4.327	12.33	0.38		4.54	4.74		2.0503	2.2349		0.69
56	62	118	0.262	−0.021	−1.046	−4.646	12.49	0.29	[4]	4.75	4.94		2.2443	2.4275		0.67
56	64	120	0.256	−0.001	−0.908	−4.908	12.63	0.25		4.79	4.98		2.2823	2.4669		0.60
56	66	122	0.253	0.012	−0.977	−5.177	12.73	0.18	0.058	4.75	4.94		2.2443	2.4275		0.52
56	68	124	0.249	0.030	−0.945	−4.845	12.84	0.20	0.029	4.61	4.81		2.1140	2.3014		0.41
56	70	126	0.247	0.046	−1.025	−4.325	12.95	0.20	0.033	4.43	4.63	4.37	1.9521	2.1324	1.9	0.30
56	72	128	0.201	0.026	−1.211	−3.311	12.96	0.02	0.031	3.70	3.93	3.7	1.3618	1.5363	1.36	0.24
56	74	130	0.169	0.019	−2.044	−2.544	13.00	0.07	0.025	2.81	3.08	3.6	0.7854	0.9436	1.29	0.15
56	76	132	0.144	0.022	−2.923	−1.123	13.06	0.11	0.018	1.38	2.17	2.94	0.1894	0.4684	0.86	0.05
56	78	134	0.007	−0.001	−4.604	−0.004	13.13	0.12	0.019	−0.08	1.47	2.614	0.0006	0.2149	0.68	0.04
58	58	116	0.272	−0.041	−1.932	−5.232	12.85	0.00		5.20	5.37		2.6897	2.8685		0.83
58	60	118	0.292	−0.035	−2.360	−6.860	13.05	0.34		5.64	5.80		3.1642	3.3462		0.88
58	62	120	0.292	−0.020	−1.808	−7.108	13.21	0.28		5.78	5.94		3.3232	3.5097		0.85
58	64	122	0.288	−0.008	−1.354	−7.154	13.34	0.22		5.82	5.97		3.3694	3.5453		0.81
58	66	124	0.290	0.010	−1.301	−7.201	13.47	0.22		5.81	5.97		3.3578	3.5453		0.73
58	68	126	0.282	0.022	−1.034	−6.634	13.59	0.21		5.68	5.85		3.2092	3.4042		0.61
58	70	128	0.266	0.045	−0.754	−5.654	13.65	0.10		5.40	5.58	4.65	2.9006	3.0972	2.15	0.42
58	72	130	0.348	0.039	−0.501	−4.201	13.76	0.19		5.18	5.40	4.18	2.6691	2.9006	1.73	0.48
58	74	132	0.182	0.024	−1.194	−3.294	13.71	−0.09		3.88	4.11	4.22	1.4975	1.6803	1.77	0.24
58	76	134	0.154	0.029	−1.973	−1.773	13.72	0.02		2.54	3.01	3.21	0.6418	0.9012	1.07	0.11
58	78	136	−0.127	0.029	−3.397	−0.497	13.76	0.07		−0.21	1.76		0.0044	0.3081		0.05
60	60	120	0.306	−0.033	−3.339	−9.039	13.71	0.00		6.33	6.46		3.9857	4.1511		0.98
60	62	122	0.309	−0.019	−2.784	−9.284	13.88	0.28		6.42	6.55		4.0999	4.2676		0.97
60	64	124	0.305	−0.005	−2.432	−9.332	14.02	0.23		6.48	6.61		4.1769	4.3461		0.90
60	66	126	0.300	0.004	−2.110	−9.110	14.17	0.25		6.46	6.60		4.1511	4.3330		0.85
60	68	128	0.305	0.012	−1.678	−8.378	14.29	0.20		6.44	6.59		4.1255	4.3199		0.80
60	70	130	0.245	0.013	−0.763	−6.863	14.40	0.18	[4]	6.34	6.48		3.9983	4.1769		0.69
60	72	132	0.339	0.032	−1.253	−6.153	14.54	0.23		6.40	6.57		4.0744	4.2937		0.69
60	74	134	0.194	0.022	−0.530	−3.830	14.49	−0.08	−0.042	5.28	5.50		2.7731	3.0090		0.47
60	76	136	0.162	0.036	−1.264	−2.264	14.43	−0.10	−0.016	3.68	4.03		1.3471	1.6155		0.20
60	78	138	−0.138	0.021	−2.446	−0.746	14.40	−0.05	0.005	−0.74	2.08		0.0545	0.4304		0.04

Tab. 1. The equilibrium features of the even-even nuclei with $50 < Z < 80$, $Z \leq N < 80$

Z	N	A	ϵ^0	ϵ_4^0	V MeV	E_{def} MeV	Q_0 b	$\partial\langle r^2\rangle$ fm^2	$\partial\langle r^2\rangle^{exp}$ fm^2	$\langle Q_2^2\rangle$ b	$\sqrt{\langle Q_2^2\rangle}$ b	Q_2^{exp} b	$B2$ e^{2}b^2	$\overline{B2}$ e^{2}b^2	$B2^{exp}$ e^{2}b^2	$\langle Q_4\rangle$ b^2
62	62	124	0.317	-0.003	-2.848	-10.248	14.53	0.00		6.87	7.01		4.6948	4.8881		0.97
62	64	126	0.314	0.009	-2.578	-10.278	14.67	0.23		6.90	7.03		4.7359	4.9160		0.90
62	66	128	0.311	0.018	-2.506	-10.406	14.81	0.23		6.89	7.03		4.7221	4.9160		0.83
62	68	130	0.313	0.030	-2.208	-9.708	14.94	0.21		6.84	6.98		4.6539	4.8463		0.77
62	70	132	0.327	0.028	-1.964	-8.764	15.07	0.21		6.84	6.98		4.6539	4.8463		0.68
62	72	134	0.342	0.039	-1.943	-7.543	15.21	0.23		6.89	7.03		4.7221	4.9160		0.71
62	74	136	0.318	0.031	-0.796	-4.796	15.26	0.08		6.33	6.52		3.9857	4.2286		0.59
62	76	138	0.180	0.035	-0.682	-2.482	15.17	-0.15		4.74	5.02	4.06	2.2349	2.5067	1.64	0.32
62	78	140	-0.154	0.023	-2.010	-1.110	15.05	-0.19	-0.116	-1.46	2.48		0.2120	0.6118		0.07
64	64	128	0.319	0.018	-2.934	-10.934	15.32	0.00		7.23	7.37		5.1997	5.4030		0.85
64	66	130	0.312	0.029	-2.952	-11.152	15.45	0.20		7.19	7.33		5.1423	5.3445		0.79
64	68	132	0.311	0.040	-2.745	-10.545	15.58	0.20		7.12	7.26		5.0427	5.2429		0.68
64	70	134	0.330	0.044	-2.530	-9.630	15.70	0.19		7.12	7.25		5.0427	5.2285		0.61
64	72	136	0.345	0.048	-2.580	-8.680	15.89	0.30		7.28	7.41		5.2718	5.4618		0.65
64	74	138	0.375	0.071	-0.501	-5.001	15.96	0.11		6.98	7.14		4.8463	5.0710		0.60
64	76	140	0.219	0.031	-0.734	-2.934	15.89	-0.11		5.57	5.81		3.0861	3.3578		0.35
64	78	142	-0.168	0.020	-1.908	-1.508	15.70	-0.30		-2.24	2.89		0.4991	0.8308		0.08
66	66	132	0.311	0.041	-3.462	-11.662	16.06	0.00		7.41	7.55		5.4618	5.6701		0.70
66	68	134	0.306	0.052	-3.391	-11.391	16.17	0.17		7.28	7.41		5.2718	5.4618		0.55
66	70	136	0.312	0.066	-3.259	-10.559	16.33	0.24		7.32	7.45		5.3299	5.5209		0.49
66	72	138	0.344	0.057	-3.160	-9.260	16.54	0.32		7.57	7.70		5.7002	5.8977		0.57
66	74	140	0.328	0.051	-1.809	-6.309	16.63	0.14		7.21	7.37		5.1710	5.4030		0.50
66	76	142	0.240	0.033	-1.110	-3.410	16.59	-0.06		6.17	6.38		3.7868	4.0489		0.32
66	78	144	-0.175	0.021	-2.198	-1.898	16.35	-0.36		-2.97	3.34		0.8774	1.1097		0.08

Z	N	A	ϵ^0	ϵ_4^0	V MeV	E_{def} MeV	Q_0 b	$\partial\langle r^2\rangle$ fm^2	$\partial\langle r^2\rangle^{exp}$ fm^2	$\langle Q_2^2\rangle$ b	$\sqrt{\langle Q_2^2\rangle}$ b	Q_2^{exp} b	$B2$ e^{2}b^2	$\overline{B2}$ e^{2}b^2	$B2^{exp}$ e^{2}b^2	$\langle Q_4\rangle$ b^2
68	68	136	0.303	0.065	−3.950	−11.550	16.83	0.00		7.53	7.68		5.6401	5.8671		0.49
68	70	138	0.300	0.081	−4.000	−11.000	16.91	0.12		7.36	7.49		5.3884	5.5804		0.28
68	72	140	0.349	0.064	−3.547	−9.347	17.18	0.40		7.98	8.13		6.3344	6.5748		0.47
68	74	142	0.314	0.058	−2.250	−6.550	17.27	0.13		7.63	7.79		5.7909	6.0364		0.42
68	76	144	0.260	0.047	−1.617	−3.717	17.26	−0.01		6.45	6.66		4.1383	4.4121		0.24
68	78	146	−0.188	0.032	−2.854	−2.454	17.03	−0.34		−3.30	3.61		1.0832	1.2963		0.07
70	70	140	0.298	0.099	−4.903	−11.303	17.55	0.00		7.48	7.63		5.5655	5.7909		0.13
70	72	142	0.356	0.071	−4.154	−9.454	17.85	0.43		8.31	8.46		6.8691	7.1194		0.37
70	74	144	0.343	0.073	−2.727	−6.427	17.93	0.11		7.97	8.15		6.3185	6.6072		0.31
70	76	146	−0.224	0.039	−2.165	−3.765	17.63	−0.43		−4.39	4.56		1.9170	2.0684		0.11
70	78	148	−0.179	0.035	−3.396	−2.396	17.67	0.06		−3.38	3.70		1.1364	1.3618		0.04
72	72	144	0.368	0.075	−4.993	−9.093	18.59	0.00		9.11	9.29		8.2554	8.5848		0.55
72	74	146	0.374	0.082	−3.649	−6.249	18.71	0.17		8.71	8.94		7.5463	7.9501		0.46
72	76	148	0.178	0.047	−2.889	−3.389	18.38	−0.46		5.39	5.70		2.8899	3.2318		0.03
72	78	150	−0.158	0.037	−4.120	−2.119	18.30	−0.11		−3.03	3.46		0.9132	1.1908		0.00
74	74	148	0.181	0.042	−3.149	−4.249	18.97	0.00		6.16	6.56		3.7745	4.2806		0.17
74	76	150	0.160	0.044	−3.940	−3.040	18.87	−0.14		4.11	4.39		1.6803	1.9170		−0.07
74	78	152	−0.140	0.042	−5.126	−1.626	18.93	0.08		−2.32	3.00		0.5354	0.8952		−0.05
76	76	152	0.144	0.045	−5.030	−2.030	19.44	0.00		2.85	3.46		0.8080	1.1908		−0.11
76	78	154	−0.133	0.044	−6.710	−1.210	19.55	0.14		−1.64	2.57		0.2675	0.6570		−0.08
78	78	156	−0.127	0.042	−8.502	−0.603	20.18	0.00		−1.02	2.09		0.1035	0.4345		−0.06

and ${}_jh_k$ is a linked matrix element of the many-body hamiltonian

$$ {}_jh_k = \langle a| \frac{\overleftarrow{\partial}}{\partial a_j} \hat{H} \frac{\overrightarrow{\partial}}{\partial a_k} |a\rangle - \langle a|\hat{H}|a\rangle \gamma_{jk} \tag{12} $$

The potential term of the collective hamiltonian $\hat{\mathcal{V}}$ consists of the two parts

$$ \hat{\mathcal{V}} = \langle a|\hat{H}|a\rangle - E_0 \tag{13} $$

where E_0, so called zero point correction is equal here

$$ \hat{E}_0 = -\frac{1}{2}\gamma_i^{ij} h_j \tag{14} $$

The expectation value of the many body effective hamiltonian (2) is evaluated within the Strutinsky [11] prescription (E_{STRUT})

$$ \langle a|\hat{H}|a\rangle \approx E_{\mathrm{STRUT}} \tag{15} $$

The Strutinsky energy reproduces well the nuclear masses and consists of the macroscopic liquid droplet E_{LD} [12] part and the shell correction $\Delta E_{\mathrm{SHELL}}$ describing the shell and pairing effects on the potential energy

$$ E_{\mathrm{STRUT}} = E_{\mathrm{LD}} = \Delta E_{\mathrm{SHELL}} \tag{16} $$

The eigen problem of the collective hamiltonian $\hat{\mathcal{H}}_{coll}$ (7) is solved by diagonalisation in the two dimensional harmonic oscillator wave functions base

$$ \hat{\mathcal{H}}_{\mathrm{coll}}\Phi_\alpha = \epsilon_\alpha \Phi_\alpha \tag{17} $$

The full many-body wave function ψ_α describing a nucleus in a state α is given within the GCM approximation by the integral:

$$ \psi_\alpha(\{x\}) = \int f_\alpha(a)|a,\{x\}\rangle da \tag{18} $$

This function will serve to calculate the dynamical values of the multipole moments. The weight function $f_\alpha(a)$ in (18) is directly connected [13] with the collective wave function Φ_α from eq. (17).

The multipole moments operators are defined as follows

$$ \hat{Q}_0 = r^2, \hat{Q}_2 = r^2\mathcal{P}_2(\cos\vartheta), \hat{Q}_4 = r^4\mathcal{P}_4(\cos\vartheta), \tag{19} $$

where r, ϑ are the single particle coordinates, $\mathcal{P}_\lambda$ — the Legendre polynomials.

It was proved in [13] that the expectation value of $\hat{Q}_\lambda$ operator between the ground state functions ψ_0 is equal to

$$Q_\lambda = \int \Phi_0^* \langle a|\hat{Q}_\lambda|a\rangle \Phi_0 da, \tag{20}$$

where the integral is evaluated in the collective space only.

In order to compare the theoretical estimates of the quadrupole moments to the experimental data, obtained from the reduced quadrupole transition probabilities $B(E2, 2^+ \rightarrow 0^+)$ [14] should use the sum rule

$$\sum_i B(E2, 2_i^+ \rightarrow 0^+) = \frac{5}{16\pi} \int \Phi_0 \hat{Q}_2^2 \Phi_0 da \tag{21}$$

where the sum goes over all the possible 2_i^+ states and is model independent. There is usually one transition $B2$ favoured in this sum [15] so it is reasonable to compare the available experimental data obtained from $B(E2)$ transitions [14] with the quadrupole moments calculated as follows

$$\langle \hat{Q}_2^2 \rangle^{1/2} = \left[\int \Phi_0^* \hat{Q}_2^2 \Phi_0 da \right]^{1/2} \tag{22}$$

The mean square radii of nuclei $\langle r^2 \rangle$ are usually not given in experiment straighty, we deal rather with the isotopic shifts of $\langle r^2 \rangle$ between various mass numbers [3,4]

$$\partial \langle r^2 \rangle = \langle r^2 \rangle^{A'} - \langle r^2 \rangle^{A} \tag{23}$$

They are related to the electric monopole moments Q_0 by

$$\langle r^2 \rangle^{Z+N} = Q_0 / Z \tag{24}$$

If the mean square radius for the magic spherical nucleus was unmeasured we took its liquid drop estimate, designing the experimental Q_0^{exp} up to this constant.

2. THE EQUILIBRIUM DEFORMATIONS, POTENTIAL ENERGIES AND MOMENTS

In the table 1 are listed: the equilibrium values of the deformation parameters ϵ^0, ϵ_4^0, potential energies $\mathcal{V}$ and deformation energies

$$E_{def} = \mathcal{V}(\epsilon^0, \epsilon_4^0) - \mathcal{V}(0,0), \tag{25}$$

Then the electric monopole moments Q_0 and the isotopic shifts of mean square radius

$$\partial\langle r^2\rangle = \langle r^2\rangle^{N+Z} - \langle r^2\rangle^{N+Z-2} \tag{26}$$

are compared with their available [3,4] experimental values $\partial\langle r^2\rangle^{exp}$. The electric quadrupole moments are calculated as $\langle\hat{Q}_2\rangle$ and $\langle\hat{Q}_2^2\rangle^{1/2}$ The second ones are closer to experimental data [14] Q_2^{exp}. The corresponding reduced quadrupole transitions

$$B2 = \frac{5}{16\pi}\langle\hat{Q}_2\rangle^2 \tag{27}$$

$$\bar{B}2 = \frac{5}{16\pi}\langle\hat{Q}_2^2\rangle \tag{28}$$

and the experimental values B2^{exp} are also presented. The hexadecapole moments Q_4 can be seen in the last column of the Table 1.

The results are printed for all the even-even combinations of $50 < Z < 80$ and $Z < N < 80$.

For the most isotopes the prolate equilibrium shapes are favoured. Only the Te nuclei and the heaviest isotopes of other elements have a chance to be oblate. The deformation energies, thanks the influence of zero point vibration to became larger by up to 1.5 MeV in our calculation, and the far from magic numbers nuclei are usually very well deformed. It means that the nonaxial γ instability in this region would be not so important as it was suggested in ref. [1].

Presented in Fig. 1 the mean square radius (points) calculated in fact up to the value of the spherical lightest isotopes radius do not reproduce well the data (crosses) in our calculation, specially their isotopic shifts show sometimes quite opposite behaviour to the experimental data. For example the theoretical shifts of the heaviest Te, Xe, Ba isotopes grow with A while their experimental values decrease. The more detailed analysis of our model is needed and will be presented in the next chapter.

In Fig. 2 [16] the quadrupole moments are drawn. The agreement with experimental data (crosses) of the $\langle\hat{Q}_2\rangle^{1/2}$ values (circules) is in general better than $\langle\hat{Q}_2\rangle$ (points) specially for Te and heavy Xe, Ba, Ce isotopes. The negative moments $\langle\hat{Q}_2\rangle$ are obtained for the heaviest Ce-Gd isotopes.

The hexadecapole moments are shown in Fig. 3. The systematic smaller values are obtained for $N = 70$, because of the shell effects.

In general the shapes of the nuclei are well described but their sizes demand the more careful description.

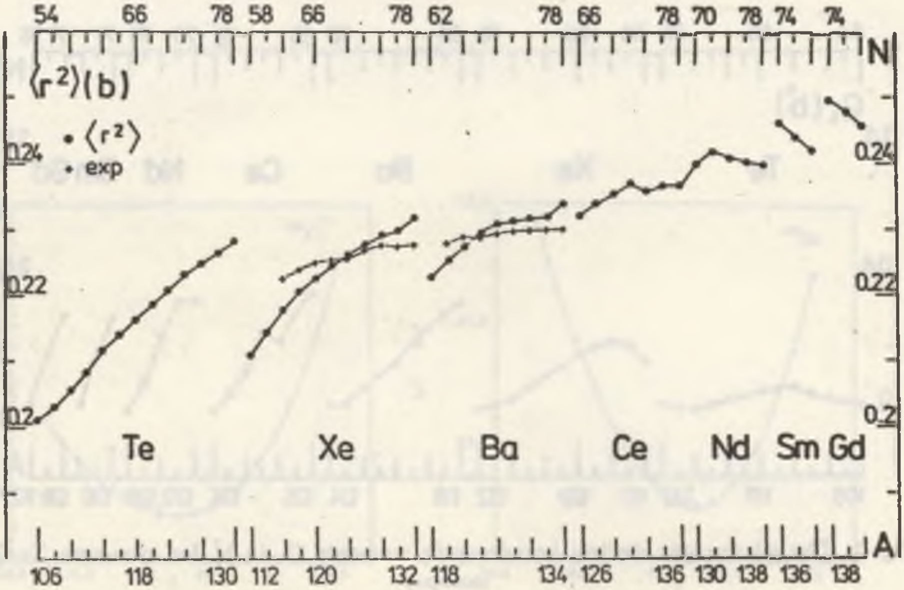

Fig. 1. The microscopic electric mean square radii $\langle r^2 \rangle$ in b (points) compared with the experimental data [4] (crosses) for even-even Te-Gd isotopes

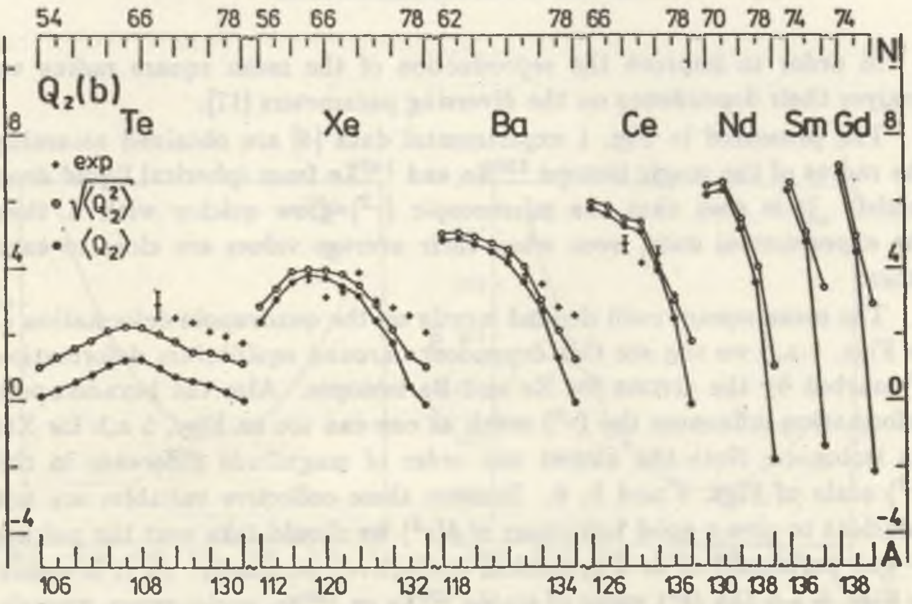

Fig. 2. The electric quadrupole moments Q_2 in b calculated as $\langle Q_2 \rangle$ (points) and $\langle Q_2^2 \rangle^{1/2}$ (circles) compared with experimental data [14] (crosses) for even-even Te-Gd isotopes

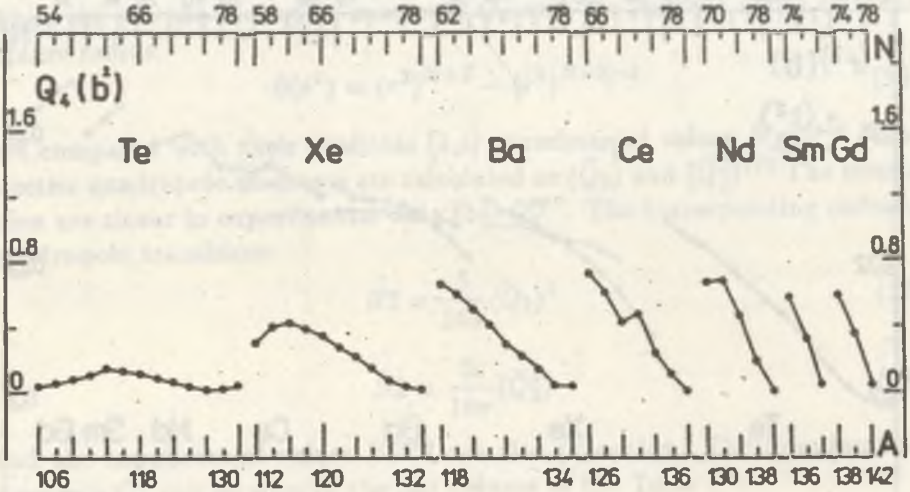

Fig. 3. The microscopic electric hexadecapole moments Q_4 in b² for even-even Te-Gd isotopes

3. THE DEPENDENCE OF MEAN SQUARE CHARGE RADII ON THE MODEL PARAMETERS

In order to improve the reproduction of the mean square radius we analyse their dependence on the diversing parameters [17].

The presented in Fig. 1 experimental data [4] are obtained assuming the radius of the magic isotope ^{132}Ba and ^{140}Xe from spherical liquid drop model. It is seen that the microscopic $\langle r^2 \rangle$ grow quicker with A then the experimental ones, even when their average values are close to each other.

The mean square radii depend mostly on the quadrupole deformation ϵ. In Figs. 4 a,b we can see this dependence around equilibrium deformation ϵ^0 marked by the arrows for Xe and Ba isotopes. Also the hexadecapole deformation influences the $\langle r^2 \rangle$ much as one can see on Figs. 5 a,b for Xe, Ba isotopes. Note the almost one order of magnitude difference in the $\langle r^2 \rangle$ scale of Figs. 4 and 5, 6. Because these collective variables are not sufficient to give a good behaviour of $\delta\langle r^2 \rangle$ we should take next the pairing — gap parameter Δ as a dynamical (collective) parameter. As it is shown in Figs. 6 a,b the $\langle r^2 \rangle$ value of stable ^{130}Xe or ^{126}Ba nuclei grows strongly with Δ.

It is almost impossible to get the values of $\langle r^2 \rangle$ and Q_2 — close to the experimental data including the ϵ, ϵ_4 parameters only. We have evaluated

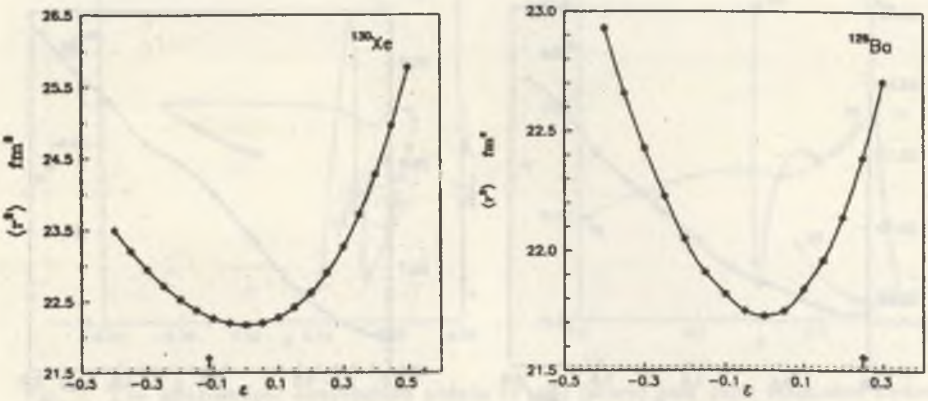

Fig. 4. The dependence of the microscopic $\langle r^2 \rangle$ in fm^2 on the quadrupole deformation ϵ for the ^{130}Xe (a) and ^{126}Ba (b) nuclei. The equilibrium deformations ϵ^0 are signed by arrows

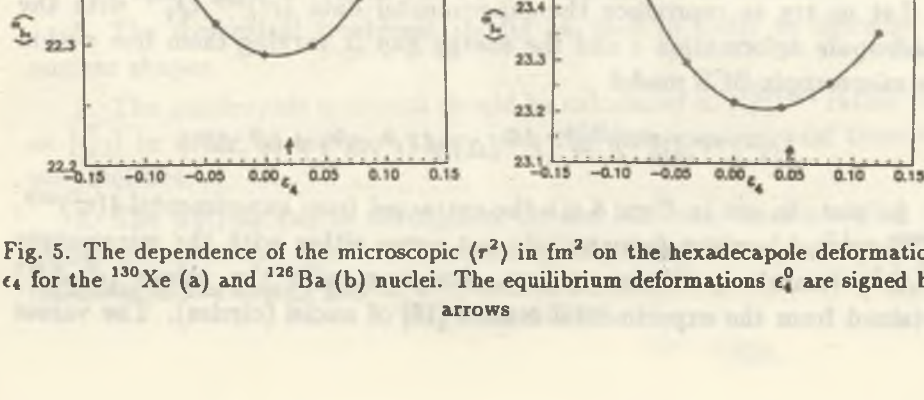

Fig. 5. The dependence of the microscopic $\langle r^2 \rangle$ in fm^2 on the hexadecapole deformation ϵ_4 for the ^{130}Xe (a) and ^{126}Ba (b) nuclei. The equilibrium deformations ϵ_4^0 are signed by arrows

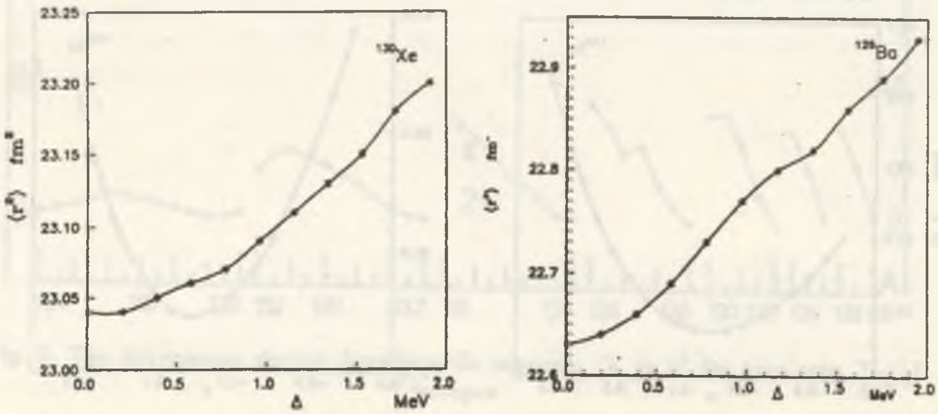

Fig. 6. The dependence of the microscopic $\langle r^2 \rangle$ in fm^2 on the pairing energy gap Δ (in MeV) for the ^{130}Xe (a) and ^{126}Ba (b)

within the liquid drop model the values of $(\epsilon^{\rm LD}\epsilon_4^{\rm LD})$ (squares in Fig. 7 a,b) which would reproduce the experimental data

$$(\langle r^2 \rangle^{exp}, Q_2^{exp}) \stackrel{\rm LD}{\rightarrow} (\epsilon^{\rm LD}, \epsilon_4^{\rm LD}) \neq (\epsilon^0, \epsilon_4^0)$$

We have assumed the favored by the microscopic calculation prolate deformation of the nucleus when solving the above equation. The solutions are far from the microscopic $(\epsilon^0, \epsilon_4^0)$ (stars in Figs. 7 a,b) equilibrium deformations both for Xe and Ba isotopes, as it is seen in Figs. 7 a,b respectively.

Let us try to reproduce the experimental data $\langle r^2 \rangle^{exp}, Q_2^{\rm exp}$ with the quadrupole deformation ϵ and the energy gap Δ varying them free within the microscopic BCS model

$$(\langle r^2 \rangle^{exp}, Q_2^{exp}) \stackrel{\rm BCS}{\rightarrow} (\epsilon^{\rm LD}, \Delta) \neq (\epsilon^0, \Delta^0) \neq (\epsilon^0, \Delta^m)$$

As you can see in Figs. 8 a,b the extracted from experimental $(\langle r^2 \rangle^{exp}, Q_2^{exp}), (\epsilon^{\rm LD}, \Delta)$ values (squares) do not agree either with the microscopic (ϵ^0, Δ^0) (stars) equilibrium points, nor even with the values (ϵ^0, Δ^m) obtained from the experimental masses [18] of nuclei (circles). The values

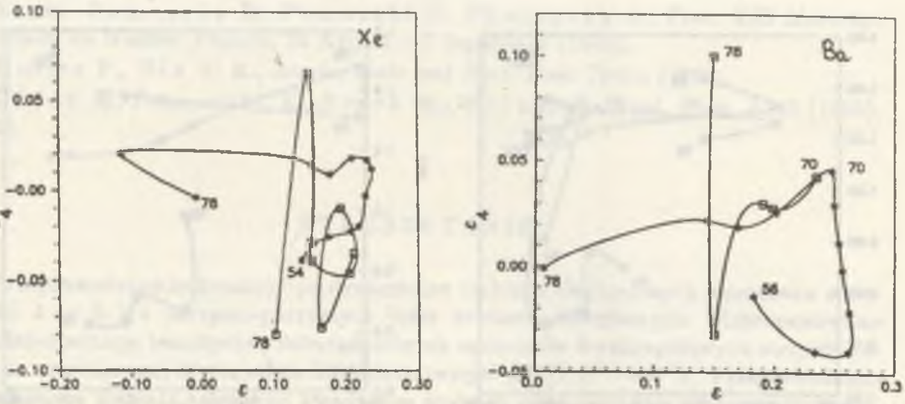

Fig. 7. The microscopic equilibrium points $(\epsilon^0, \epsilon_4^0)$ (stars) and their estimates deduced from the experimental values of $(\langle r^2\rangle^{exp}, Q_2^{exp})$ [3,4,14] within the liquid drop model $(\epsilon^{LD}, \epsilon_4^{LD})$ (squares) for the Xe (a) and Ba (b) isotopes

of Δ which reproduce the experimental $\langle r^2\rangle^{exp}$ and Q_2^{exp} are almost half of their estimates from masses Δ^m It is necessary to use the dynamical pairing model [19] which would give the most probable Δ values smaller than the equilibrium value corresponding to the minimal potential energy. Such calculation is prepared now.

CONCLUSION

The following conclusions can be drawn from our calculations:

1. The dynamical treatment should be used in order to describe the nuclear shapes.

2. The quadrupole moments should be calculated as $\langle \hat{Q}_2^2\rangle^{1/2}$ rather than as $\langle \hat{Q}_2\rangle$ in order to compare them with the data experimental transition probabilities.

3. The nuclear radius description for the far from the β stability line nuclei demands the dynamical treatment of pairing forces, especially the inclusion of the energy gap as a dynamical variable.

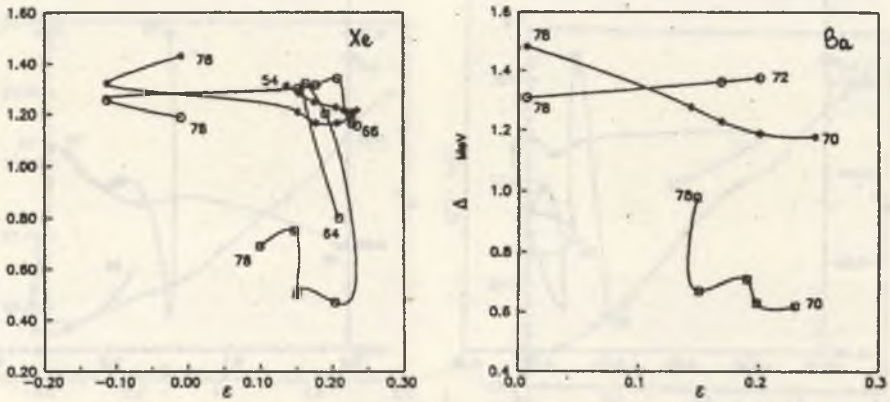

Fig. 8. The microscopic values of (ϵ^0, Δ^0) (stars) compared with the evaluated from experimental masses (ϵ^0, Δ^m) (circles) and the (ϵ^{LD}, Δ) (squares) reproducing in microscopic model the experimental $(\langle r^2\rangle^{exp}, Q_2^{exp})$ for Xe (a) and Ba (b) isotopes

REFERENCES

1. Arseniev D.A., Sobiczewski A., Soloviev V.G., *Nucl. Phys.* A126 (1969), 446.
2. Nerlo-Pomorska B., *Nucl. Phys.* A259 (1976), 481.
3. Aufmuth P., Heilig K., Steudel S., *Atomic Data and Nuclear Data Tables* 37 (1987), 455.
4. Otten E.W., *Treatise on Heavy Ion Science*, Vol. 8 (1989).
5. Nerlo-Pomorska B., Pomorski K., *Annales UMCS, Sec. AAA*, 43/44, 21 (1988/89), 211.
6. Seo T., *Z. Phys.* A324 (1986), 43.
7. Nerlo-Pomorska B., *Z. Phys.* A328 (1987), 11.
8. Góźdź A., Pomorski K., *Nucl. Phys.* A451 (1986), 1.
9. Piłat S., Pomorski K., Staszczak A., *Z. Phys.* A332 (1989), 259.
10. Bohr A., Mottelson B.R., *Nuclear Structure*, Vol. 2, Benjamin, New York 1975.
11. Strutinski V.M., *Nucl. Phys.* A95 (1967), 420.
12. Myers W.D., Świątecki W.J., *Ann. Phys. N.Y.* 84 (1974), 186.
13. Nerlo-Pomorska B., Pomorski K., Brack M., Werner E., *Nucl. Phys.* A462 (1987), 252.
14. Raman S., Matarkey C.H., Milner W.I., Nestor C.W, Stelson P.H, *Atomic Data and Nucl. Data Tables* 36/1 (1987), 1.

15. Rohoziński S. G., Dobaczewski J., Nerlo-Pomorska B., Pomorski K., Srebrny J., *Nucl. Phys.* A292 (1977), 66.
16. Nerlo-Pomorska B., Pomorski K., Skorupska B., *Proc. XXV Zakopane School of Physics*, 5–12 May (1990).
17. Nerlo-Pomorska B., Pomorski K., Skorupska B., *Proc. XXI Masurian School on Nuclear Physics*, 26 August – 5 September (1990).
18. Moller P., Nix J. R., *Atomic Data and Nucl. Data Tables* (1986).
19. Góźdź A., Pomorski K., Brack M., Werner E., *Nucl. Phys.* A442 (1985), 50.

STRESZCZENIE

Przeprowadzono mikroskopowe dynamiczne rachunki elektrycznych momentów o połowości $\lambda = 0, 2, 4$ parzysto-parzystych jąder neutrono-deficytowych. Zaproponowano nową interpretację teoretyczną doświadczalnych momentów kwadrupolowych otrzymywanych ze zredukowanych prawdopodobieństw przejść $B(E2, 2^+ \rightarrow 0^+)$. Przeprowadzono dokładniejsze badania zależności kwadratów średnich promieni jąder od parametrów deformacji wyższych multipolowości i oddziaływania „pairing”.